Trans. of the Society of Instrument and Control Engineers
Vol. E-1, No. 1, 1/9 (2001)

Theoretical Study on the Surface Force in Microstructures

Shigeki TSUCHITANI*, Seiko SUZUKI**, Masahiro MATSUMOTO**, and Masayuki MIKI***

In microstructures such as microsensors and microactuators, a smal attractive force can occur between two contacting surfaces which affects their operations. Therefore, it is very important to clarify the generation mechanism of this surface force and to find a way to decrease it in order to realize these devices. In this study, the surface force between two contacting surfaces in a sample microstructure was evaluated theoretically and the force magnitudes obtained were compared with the measured values which we reported previously. Four kinds of basic physical forces, i.e. van der Waals force; capillary force due to capillary condensation of water molecules from the humid environment, hydrogen bonding force between adsorbed water molecules, and electrostatic force baed on a contact electrification were calculated by modeling the contacting parts in the sample. The sample microstructure has a movable plate supported by a cantilever beam and two counter fixed electrodes. The movable plate and one of the fixed electrodes contacts each other when the movable plate is displaced significantly. We found that the van der Waals force, the capillary force and the hydrogen bonding force could generate surface force magnitudes which were in the range of the measured force value. From the theoretical analyses and the earlier experimental results, we concluded that the dominant surface force in usual microstructures is the capillary force due to the capillary condensation of the water when the relative humidity of the environment is higher than about 60%; it is hydrogen bonding force between water molecules adsorbed on the two surfaces when the humidity is relatively low; and it is the van der Waals force when physisorbed water molecules on the surface are almost moved out.

Key Words : microstructure, microsensor, microactuator, surface force, van der Waals force, capillary force, hydrogen bonding force, electrostatic force

1. Introduction

In microstructures such as microsensors and microactuators fabricated by semiconductor micromachining technologies, surface areas per unit volume are larger compared with those in conventional macroscopic structures. Further, when movable parts in the micromachined structures contact with counter parts separated by small gaps, contact areas per unit surface area are usually larger than those in the macroscopic structures, since the surfaces of the microstructures are usually smoother. Therefore, in the microstructures, interactions between the surfaces are relatively large compared with gravitational force and inertia force which are proportional to the volume and the surface force plays important roles in their fabrication processes and in their operations.

For example, in some microstructures fabricated by surface micromachining technologies, they couldn't operate because their movable parts adhered to counter parts separated by small gaps by the surface force[1),2)]. Further, in micro motors formed on substrates, friction forces between rotors and the substrates which were greatly affected by the surface force between them had large influences on their operation such that they determine the maximum rotating speed. Therefore, to clarify the generation mechanism of the surface force and to find a way to reduce it is very important to realize these microscopic devices which have the movable parts.

By measurements of the surface force using a sample microstructure fabricated by the silicon unisotropic etching technology, we already confirmed that the surface force could be decreased by surface treatments to reduce adsorption of water molecules from environment, such as a heating of the structure and a surface modification to achieve hydrophobic surfaces. This means that the interaction force between thin water films on the surfaces have a large contribution to the surface force.

In this paper, we calculate the magnitudes of the surface forces generated by various basic physical forces in the sample microstructure and analyze the generation mechanism of the surface force in the microstructure by comparing the calculated values with the measured one obtained by our previous experiment.

2. Microstructure for surface force analysis and various physical forces

2.1 Microstructure for surface force analysis

Fig.1 shows a cross section of a device used in our previous

* Intellectual Property Office, Hitachi Ltd., Hitachi-shi, Ibaraki (Currently, Fuculty of Systems Engineering, Wakayama University, Sakaedani, Wakayama-shi, Wakayama)
** Hitachi Research Laboratory, Hitachi Ltd., Oomika-cho, Hitachi-shi, Ibaraki
*** Automotive Product Group, Hitachi Ltd., Takaba, Hitachinaka-shi, Ibaraki

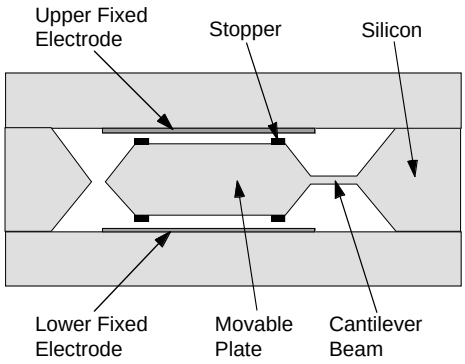

Fig. 1 Cross section of microstructure to evaluate surface force

measurement of the surface force[5]. A rectangular movable plate (length: 1300μm, width: 1800μm, thickness: 200μm) supported by a cantilever beam was formed by the silicon anisotropic etching. On upper and lower sides of the movable plate, counter fixed electrodes of molybdenum thin films (thickness: 0.3μm) were formed on insulator substrates. A gap width between the movable plate and each of the fixed electrode was 3μm when the displacement of the movable plate was zero. To avoid direct electrical contacts of the movable plate with the fixed electrodes when the movable plate displaced largely, square SiO_2 thin films (150μm x 150μm x 0.4μm) which were called stoppers were formed at each corner on the upper and the lower surfaces of the movable plate. Accordingly, the movable plate could contact with the fixed electrodes through the stoppers. Especially, when the surface force between the stoppers and the fixed electrodes is not so large, only two stoppers at the tip of the movable plate contact with the fixed electrodes. In this state, the angle θ between the surface of the fixed electrode and the counter surface of the movable plate or the stopper surface is about 0.0012rad.

Figs.2,3 show the surfaces of the SiO_2 stopper and the fixed electrode observed by a scanning electron microscope (SEM). The stopper surface is much smooth compared with that of the fixed electrode. **Fig.4** shows a topographic image of the fixed electrode observed by an atomic force microscope (AFM). From the image of the AFM, the amplitude h and the period λ of the surface roughness of the fixed electrode are from 10nm to 20nm and from 100nm to 200nm, respectively.

In the previous experiment, when the stoppers at the tip of the movable plate adhered to the fixed electrode, the surface force between them was from 1.6×10^{-5}N to about 1.5×10^{-4}N.

2.2 Various physical forces

In powder technology, objects of studies are micro substances (powder particles) as well as those in the field of the microsensors and the microactuators. Since the surface force between the powder particles has influences on various macroscopic properties of the powder, many studies on the surface force have been carried out.

Fig. 2 SEM photograph of surface of the stopper formed on the movable plate

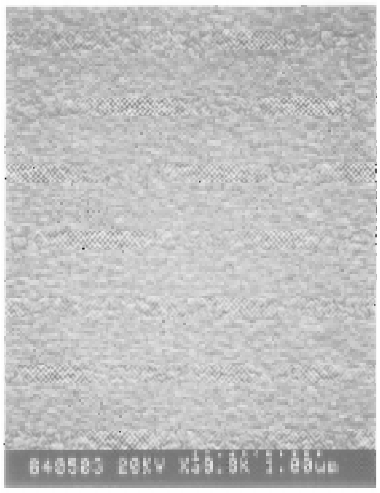

Fig. 3 SEM photograph of surface of the fixed electrode

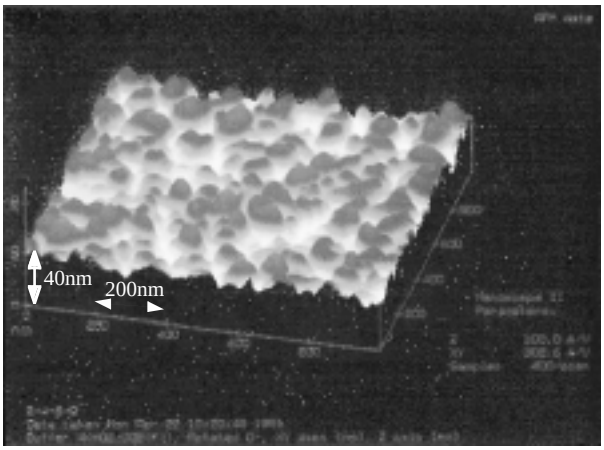

Fig. 4 AFM (Atomic Force Microscope) image of surface of the fixed electrode

According to this technology, the basic physical forces working between the surfaces of the small powder particles are van der Waals force, capillary force and electrostatic force, which are explained below.

(1) Van der Waals force

The van der Waals force is a kind of electrostatic interactions which acts between molecules or atoms and also works between two macroscopic bodies such as particles and walls when they approaches each other extremely. The van der Waals force between the SiO_2 stopper and the molybdenum fixed electrode in Fig.1 is generated by dispersion force since both SiO_2 and molybdenum are non-polar. The dispersion energy E_A between the same kinds of molecules or atoms which are electrically neutral and symmetry is approximated as follows[8]:

$$E_A = -\beta_{11}/r^6 \ , \tag{1}$$

where r is the distance between the centers of the molecules or the atoms and β_{11} is London constant. London constant β_{12} for the dispersion energy between different kinds of molecules is approximated as follows using London constants β_{11} and β_{22} for same kinds of molecules:

$$b_{12} = \sqrt{\beta_{11}\beta_{22}} \ . \tag{2}$$

According to Hamaker's theory, the dispersion energy between two separated macroscopic bodies is calculated by adding all interactions among all molecules included in them, i.e. the van der Waals potential energy is calculated by the next equation [9]:

$$E = -\int_{v_1}\int_{v_2} \frac{q_1 q_2 \beta_{12}}{r^6}\, dv_1 dv_2 \ , \tag{3}$$

where v_1 and v_2 are the volumes of the two bodies , dv_1 and dv_2 are the volume elements of the two bodies and q_1 and q_2 are the numbers of the molecules per unit volume in the two bodies. The van der Waals force is almost independent of environmental conditions.

(2) Capillary force

Liquid films existing at contacting parts or narrow gaps between two solids is called liquid bridges. In humid environments, the liquid bridges are formed by capillary condensations of water vapor in the environment to the gaps around the contacting part between the solids. A force generated by the liquid bridge, i.e. a capillary force is affected by the amount of the condensed water and the shape of the liquid bridge, which depend on the environmental humidity, affinities of the solid surfaces for the water (hydrophilicity), the shape of the contacting part and the contacting condition.

When the liquid bridge is formed at the contacting part of same sizes of spherical particles as shown in **Fig.5**, the capillary force F working between the two particles is obtained by adding a force F_C due to a pressure deficiency within the liquid and a force F_S due to a surface tension at the narrowest part (neck) of the liquid bridge. When the surface force due to the capillary force is calculated the liquid is usually treated to have same physical properties as those

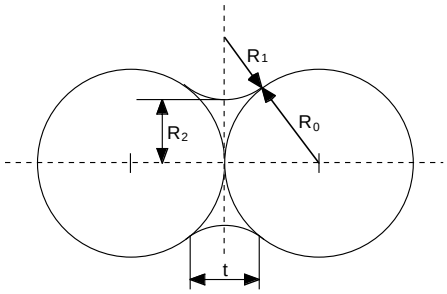

Fig. 5 Liquid bridge formed between two spherical particles

of the bulk liquid. However, in very thin liquid films, their physical properties are different from those of the bulk liquid due to interactions with the solid surface. According to studies in the powder technology, the water films formed on the solid surfaces have the properties of the liquid in the relative humidity higher than about 60% and the capillary condensation is possible in this humidity region. The thickness of the condensed water film in this critical humidity is from 2.9nm to 3.7nm[7), 11)]. Therefore, when we calculate the surface force generated by the adsorbed water in the humidity less than about 60%, it is necessary to consider directly the hydrogen bonding force which is the main attraction force between the water molecules. When two flat silicon substrates are bonded in the room temperature in the silicon to silicon direct bonding, they adhere by the force from $3\times10^5 N/m^2$ to $5\times10^5 N/m^2$. This adhesion force is considered to be generated by the hydrogen bonding force[12].

(3) Electrostatic force

The electrostatic attraction force is generated by transfers of charge carriers (mainly electrons) between the two contacting bodies. The driving force of the charge transfer is the difference of the electro chemical potentials of the two materials. As a result of the charge transfer, electric double layers are formed at the contacting part, i.e. two counter surfaces are electrically charged to opposite signs each other (contact electrification). When the initial electro chemical potential difference between the two materials is supplemented by the electric potential difference in the electric double layers, the charge transfer stops.

In the contact of the insulator and the metal such as that of the SiO_2 stopper on the movable plate and the fixed electrode in Fig.1, the amount of the electrification is determined by the work function of the metal and that of the insulator from its surface energy levels and its trap energy levels. The charge density σ [C/m^2] of the electric double layer generated by the contact of the insulator and the metal is expressed as follows:

$$\sigma = \frac{W_i - W_m}{\dfrac{1}{eN_s + \sqrt{\varepsilon N_b}} + \dfrac{ed}{\varepsilon_0}} \ , \tag{4}$$

where W_i and W_m [eV] are the work functions of the insulator and the metal, respectively and N_s [1/(eVm^2)] is the density of the surface energy levels of the insulator, N_b [1/(eVm^3)] is the density of the trap energy level in the insulator, d is the distance between the surfaces of the insulator and the metal, which is about 4 Å and ε and ε_0 are the dielectric constants of the insulator and the vacuum, respectively.

3. Theoretical study of surface force generated by various physical forces

In this chapter, the magnitudes of the surface forces due to four kinds of physical forces described in the above are evaluated theoretically by modeling the device shown in Fig.1 and the calculated values of the surface force are compared with the measured values already obtained. In the investigation, only the surface force between the stoppers at the tip of the movable plate and the fixed electrode is analyzed.

3.1 Surface force due to van der Waals force

To calculate the van der Waals force between the stoppers and the fixed electrode, we model the vicinity of the contacting part as shown in the cross section of **Fig.6**. That is, we simlify the contact portion in the next ways.

(a) From the SEM photographs (Figs.2,3) and the AFM image (Fig. 4), the stopper surface is much smoother than the surface of the fixed electrode. So, we asuume that the stopper surface is a plane (x-y plane) and the surface roughness exists only on the fixed electrode. To express the surface roughness of the fixed electrode, we regard the density of the fixed electrode as depending on the depth (z co-ordinates) from the surface and beingsame in the same depth, i.e. the density is averaged within each plane parallel to the surface. As the simplest case, we express the fixed electrode with the surface roughness of the amplitude of h as follows: the density ρ increases linearly to the depth of h with increasing the depth and is constant ρ_0 in the place deeper than h.

(b) Since the thickness of the stopper and that of the fixed electrode are enough large compared with the range where the van der Waals force is effective (several times of the diameter of the molecule), we regard the fixed electrode as extending infinitely under its surface. Further, we consider that the stopper shown in Fig.6 is surrounded by two planes passing through straight lines OA and OB and perpendicular to the surface of the paper and the width of the stopper in the direction perpendicular to the paper is l. Since the surface area of the fixed electrode is enough large compared with that of the stopper, we regard the fixed electrode as extending infinitely to x and y directions.

By executing the integration of eq.(3), the van der Waals potential energy E is calculated as follows:

$$E = -\frac{Hl}{12\pi}\left\{\frac{1}{\tan\theta} - \frac{1}{\tan(\theta+\phi)}\right\}\frac{1}{h}\ln\left(1+\frac{h}{d}\right), \qquad (5)$$

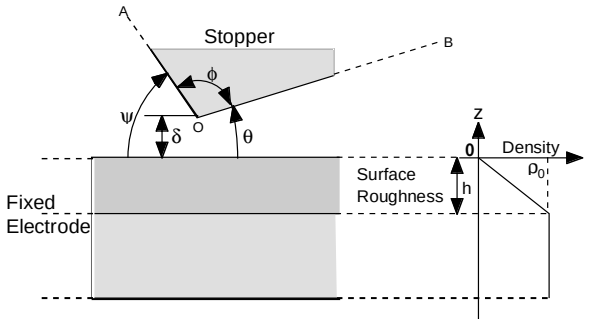

Fig. 6 Schematic for the calculation method of van der Waals force between the stopper nad the fixed electrode

where ϕ is the angle between the lines OA and OB, θ is the angle between the stopper surface passing through the line OB and the surface of the fixed electrode and d is the distance between the surface of the fixed electrode and the tip of the stopper (a line perpendicular to the paper through point O). H is Hamaker constant calculated by the next equation using Hamaker constants H_{11} and H_{22} of the materials of the stopper and the fixed electrode when the medium between them is vacuum or air:

$$H=H_{12}=\sqrt{H_{11}\cdot H_{22}}\ . \qquad (6)$$

When a medium with Hamaker costant H_{33} is filled between the stopper and the fixed electrode, Hamaker constant H is calculated as follows[7]:

$$H=H_{132}=(\sqrt{H_{11}}-\sqrt{H_{33}})(\sqrt{H_{22}}-\sqrt{H_{33}})\ , \qquad (7)$$

where Hamaker constant H_{ii} (i=1, 2, 3) is expressed as follows using London constant β_{ii} :

$$H_{ii}=\pi^2 q_i^2 \beta_{ii}\ .$$

The measured Hamaker constants are in the ranges from 15x10^{-20}J to 50 x10^{-20}J for metals, from 6 x10^{-20}J to 15 x10^{-20}J for oxides and 4 x10^{-20}J for water[7].

From eq.(5), the van der Waals force F_{vdw} is calculated as follows:

$$F_{vdw} = -\left.\frac{\partial E}{\partial d}\right|_{d=\delta}$$

$$= -\frac{Hl}{12\pi}\left\{\frac{1}{\tan\theta} - \frac{1}{\tan(\theta+\phi)}\right\}\frac{1}{\delta(\delta+h)}\ , \qquad (8)$$

where δ is the distance having the minimum potential energy and determined by the van der Waals force and Born's repulsive force. Usually δ is about 4Å in air. In the numerical calculation of the surface force generated by the van der Waals force by eq.(8), as Hamaker constants of the stopper (SiO_2) and the fixed electrode (Mo), Hamaker constants for the oxides and the metals described in the above were used. Further, we put l=150μmx2=300μm and θ=0.0012rad as described in the explanation of the device structure and $\phi=\pi/2$rad assuming that the stoppers have side walls perpendicular to the stopper surface.

Fig.7 shows the surface roughness (h) dependences of the surface force generated by the van der Waals force calculated using eq.(8) when the stoppers and the fixed electrode contact each other, i.e.

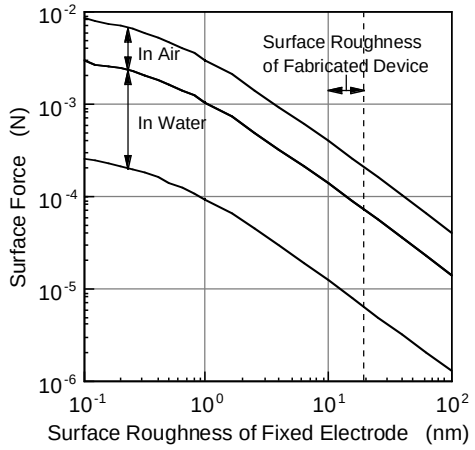

Fig. 7 Surface force due to the van der Waals force between the movable plate and the fixed electrode as a function of surface roughness of the fixed electrode

they are placed with the very small spacing δ between them. The area between the upper and the middle curves is the range of the van der Waals force in air or in vacuum and that between the middle and the lower curves is the force range in the water. In the figure, the range of the measured surface roughness of the fixed electrode (10-20nm) is drawn.

The calculated value of the van der Waals force in air or in vacuum is from 7×10^{-5}N to 4×10^{-4}N. This force range overlaps with that obtained by the measurement (from 1.6×10^{-5}N to 1.5×10^{-4}N). When the surface roughness h is much larger than δ, the van der Waals force decreases being inversely proportional to h from eq.(8).

On the other hand, the calculated van der Waals force in the water is from 6×10^{-6}N to 1.5×10^{-4}N and less than that in air or in vacuum. That is, the water between the stoppers and the fixed electrode has a shield effect for the van der Waals force between them. This means that the van der Waals force decreases by the capillary condensation of the water to the contacting part of the stoppers and the fixed electrode.

In case of $\theta<<\phi$ and $\theta<<\psi$, eq.(8) is approximated as follows:

$$F_{vdw} = -\frac{Hl}{12\pi\tan\theta}\cdot\frac{1}{\delta(\delta+h)} \quad . \tag{9}$$

According to eq.(9), the van der Waals force is independent of the tip angle ϕ of the stopper which is influenced by the fabrication process and the fabrication condition.

3.2 Surface force due to water layer on surface

We calculate the capillary force due to the capillary condensed water to the contacting part of the stoppers and the fixed electrode from the humid environment. Further, we estimate the surface force generated by the hydrogen bonding force between the water molecules adsorbed on the surfaces.

(1) Capillary force

We model the vicinity of the contacting part as shown in **Fig.8**.

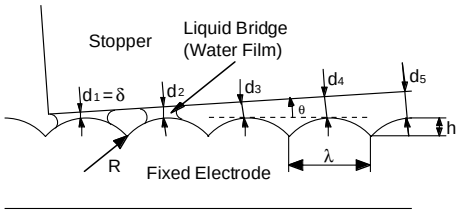

Fig. 8 Schematic for the calculation method of the capillary force between the stopper and the fixed electrode

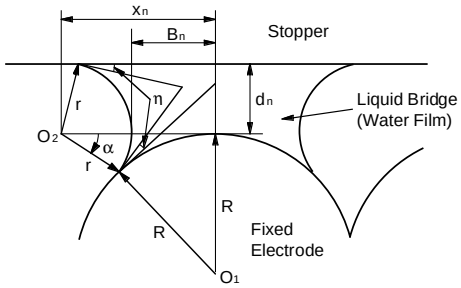

Fig. 9 Schematic for the calculation method of the capillary force between the stopper and a sherical projection on the surface of the fixed electrode

We express the surface roughness of the fixed electrode as an array of spherical projections, i.e. the spherical projections with a radius R and a height h are arranged on the surface of the fixed electrode in a manner that their summits form a square lattice with a period λ.

Fig.9 shows the liquid bridge (water film) formed between one spherical projection on the fixed electrode and the stopper. The total surface force is calculated by adding the capillary forces between the stopper and all of the projections where the formations of the liquid bridge are possible. To calculate the capillary force, we further put the next assumptions.

(a) The outline of the surface of the liquid bridge (cross line with a plane including the line drawn from the top of the sphere to the fixed electrode perpendicularly) is a part of a circle with a radius r (radius of capillary condensation).

(b) Contact angles of the water with the surfaces of the stopper and the fixed electrode are both η.

(c) When forces to separate the stopper and the projection in opposite directions are applied to them, the expected line where the cutting of the liquid occurs is the line along the narrowest part (neck) of the liquid bridge.

(d) Layers of the adsorbed water molecules on the surface of the stopper and the fixed electrode are not taken into consideration (adsorbed water layers on solid surfaces are usually from 2 to 4.5 molecular layers, i.e. their thicknesses are from 0.58nm to 1.3nm[7]).

The radius R of the spherical projection is given by the next equation using the height h of the projection and the distance λ between their summits.

$$R=\frac{1}{2h}\left(\frac{\lambda^2}{4}+h^2\right) \tag{10}$$

Using the angle θ between the envelope of the projections and the stopper, the distance d_n between the n-th projection (Fig.8) and the stopper is calculated as follows:

$$d_n = (n-1)\lambda\sin\theta + (R+\delta)\cos\theta - R \ , \tag{11}$$

where δ is the nearest distance between the projections and the stopper. In Fig.9, the distance x_n between the normal line of the stopper surface passing through the center O_1 of the sphere and the center O_2 of the circle which is the outline of the liquid bridge is given by the next equation by a simple geometrical calculation:

$$x_n = \sqrt{R^2+r^2+2Rr\cos\eta-(R+d_n-r\cos\eta)^2} \ . \tag{12}$$

The radius B_n of the narrowest part of the liquid bridge is give by the following equations:

$$\begin{aligned} B_n &= x_n - r\cos\alpha \quad (\text{for } a\geqq 0) \ , \\ B_n &= x_n - r \qquad\quad (\text{for } a<0) \ , \end{aligned} \tag{13}$$

where α is the angle between the stopper surface and a straight line connecting the point O_2 with a point on the contact line of the liquid bridge and the projection. A force F_{cn} due to the pressure deficiency inside the liquid and the surface tension F_{sn} in the expected line where the cutting occurs are calculated as follows:

$$\begin{aligned} F_{cn} &= \pi B_n^2\sigma\left(\frac{1}{R}-\frac{1}{B_n}\right) \ , \\ F_{sn} &= 2\pi B_n\sigma \ , \end{aligned} \tag{14}$$

where σ is the surface tension of the water (0.0727N/m). The capillary force F_n between the n-th projection and the stopper is give by the next equation:

$$F_n = F_{cn} + F_{sn} \ . \tag{15}$$

The total surface force generated by the liquid bridge between the fixed electrode and the stopper is calculated by adding F_n over all projections where the formations of the liquid bridges are possible.

On the other hand, parameters R_1 and R_2 to express the shape of the liquid bridge formed between two spheres shown in Fig.5 can be estimated by the next Kelvin's equation of the capillary condensation:

$$\ln(rH) = -\frac{(M/\rho L)\sigma\cos\theta}{\boldsymbol{R}T}\left(\frac{1}{R_1}+\frac{1}{R_2}\right) \ , \tag{16}$$

where rH is the relative humidity of the environment, M is the molecular weight of the water (18×10^{-3}kg/mol), R_1 and R_2 are radiuses of curvature (when the liquid bridge is convex, the sign is negative) when the liquid bridge is cut by two planes perpendicular each other, $\boldsymbol{R}$ is the gas constant (8.314JK/mol) and T is the absolute temperature. When the thickness of the liquid bridge is enough smaller than the radiuses of the spheres, R_1/R_2 is approximated as $-\infty$ because the shape of the liquid bridge is regarded as a thin disk, and eq.(16) is transformed into eq.(17).

$$\ln(rH) = -\frac{(M/\rho L)\sigma\cos\theta}{\boldsymbol{R}TR_1} \tag{17}$$

By setting $r=R_1$ in eqs.(13) and (14), the humidity dependence of the capillary force due to the capillary condensation of the water is calculated.

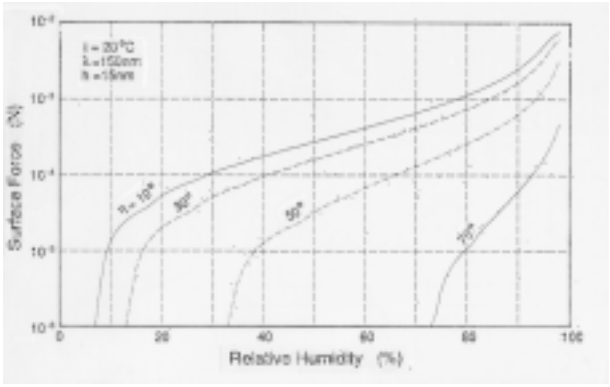

Fig. 10 Surface force due to the capillary force between the movable plate and the fixed electrode as a function of relative humidity for different contact angle of water

Fig.10 shows relative humidity vs. surface force curves for various contact angles η of the water in case of h=15nm and λ=150nm (cf. Fig.4). The surface force depends on the humidity remarkably and increases with increase of the humidity. The force is also influenced by the contact angle η of the water to the surfaces of the fixed electrode and the stopper and are larger for the surfaces with smaller contact angles, i.e. more hydrophilic surfaces. The contact angle of the water to metals are zero or very small in the usual metals with thin surface oxide layer[15]. The contact angle of the water to quartz (SiO_2) is also almost zero.

When the contact angle η is 10 degrees in Fig.10, the calculated surface force is from 3×10^{-4}N to 4×10^{-4}N in the humidity from 50% to 60% which is almost same as the humidity in the environment where the surface force measurement was carried[5]. This value of the surface force is near to the maximum value (1.5×10^{-4}N) of the measured surface force.

Therefore, the observed surface force also can be explained by the capillary force due to the capillary condensation of the water into the contacting parts of the fixed electrode and the stoppers.

Fig.11 shows the influences of the surface roughness, i.e. the height of the projections of the fixed electrode on the surface force generated by the capillary force. The higher the projection height is, i.e. the larger the surface roughness of the fixed electrode is, the smaller the surface force becomes. Therefore, the enlargement of the surface roughness of the contacting part is one of the effective ways to reduce the surface force due to the capillary force as well as in the case of the van der Waals force.

(2) Hydrogen bonding force

As described in § 2.2, the capillary condensations of the water

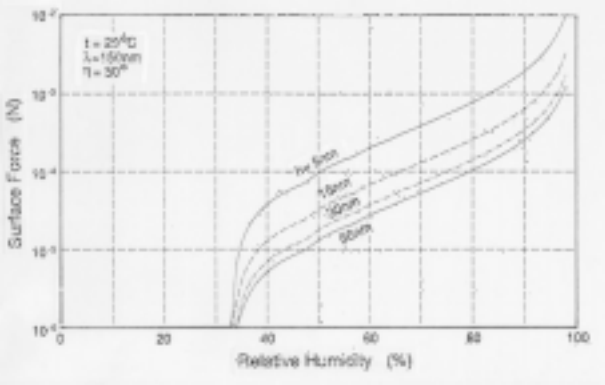

Fig. 11 Surface force due to the capillary force between the movable plate and the fixed electrode as a function of relative humidity for different height of the projection on the surface of the fixed electrode

to the small gap between the solids were usually observed in the relative humidity higher than about 60%[7),11)], although this threshold humidity is a little different depending on the materials of the solids. Therefore, in the low humidity condition it is necessary to estimate the surface force generated by the surface water layer in other way, i.e. we calculate the surface force directly taking the hydrogen bonding force between the water molecules into consideration.

In the calculation of the surface force generated by the hydrogen bonding force, we model the contacting part in the same way as in the calculation of the surface force due to the capillary force, i.e. the surface of the fixed electrode is covered by many spherical projections and the stopper surface is smooth like a plane.

The thickness of the liquid bridge in the humidity of about 60% above which the formation of the liquid bridge of the water is possible is from 2.9nm to 3.7nm[7),11)]. Therefore, in the calculation of the surface force due to the hydrogen bonding force, we suppose that the maximum thickness t_c of the water film formed in the gap between the stopper and the fixed electrode is in this range. Further, we think that the formation of the water film which contributes to the surface force is possible in the portions where the distance d between the projection on the fixed electrode and the stopper is less than t_c as show in **Fig.12**. In the n-th spherical projection, the area where such a thin water film is formed is a circle with the radius r_n which is give by the next equation:

$$r_n = \sqrt{2R(t_c - d_n) - (t_c - d_n)^2} \quad , \tag{18}$$

where d_n is the distance between n-th projection and the stopper and given by eq.(11).

On the other hand, from the measurement in the silicon to silicon direct bonding, the surface force generated by the hydrogen bonding force between very smooth (mirror polished) surfaces is considered to be from 3×10^5N/m^2 to 5×10^5N/m^2 [12)]. Further, we suppose that the surface force between two surfaces generated by the hydrogen bond of the intermediate water layer is independent of the distance

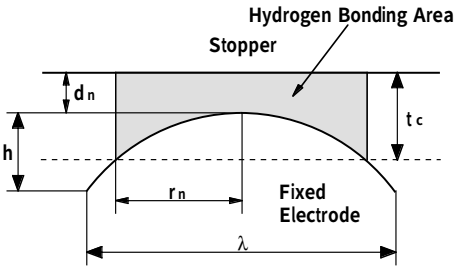

Fig. 12 Hydrogen bonding area between the stopper and a spherical projection on the surface of the fixed electrode

between the surfaces, since three dimensional hydrogen bond is possible between the water molecules.

The total surface force between the stoppers and the fixed electrode is calculated by the product of the hydrogen bonding force per unit area and the total area where the water films which contribute to the surface force are formed. The total area of such water films is obtained by adding the areas of the circles with the radius given by eq.(18) over all projections where the water films are formed.

When the height h of the projections is 15nm, the period λ of the projection array is 150nm and the maximum thickness of the water layer is t_c (2.9-3.7nm) as described in the above, the maximum of the surface force generated by the hydrogen bonding force in the fabricated microstructure was estimated to be from 1.4×10^{-5}N to 3.9×10^{-5}N.

Since this calculated surface force range is almost included in the range of the measured surface force (from about 1.6×10^{-5}N to 1.5×10^{-4}N), the hydrogen bonding force can also explain the experimental results about the surface force magnitude.

3.3 Surface force due to electrostatic force

We estimate the electrostatic force due to the contact electrification of the stopper and the fixed electrode. In eq.(4), $W_i - W_m$ is the difference of the Fermi levels of the insulator and the metal, and $(W_i - W_m)/e = V_c$ is the contact potential difference between them, where e is the electric charge of the electron. When the density N_s of the surface level of the insulator is so large as to satisfy the relation $N_s >> \varepsilon_0/e^2 d$, eq.(4) is simplified as follows:

$$\sigma = \varepsilon_0 V_c / d \quad , \tag{19}$$

where d is the distance between the two objects. Magnitude of the contact potential difference V_c is usually less than 1V.

We calculate the electrostatic force due to the contact electrification based on eq.(19). We also suppose that the surface of the fixed electrode is covered by the spherical projections and the surface of the stopper is smooth like a plane.

When two objects contact each other, the electron transfer between them takes place by the tunneling effect. The electron flow due to the tunneling decreases rapidly in the surface distance

between 10Å and 15Å. According to Harper, this critical distance d_c is 12.7Å. The electron transfer due to the tunneling effect is possible in the areas where the distance between the surface of the projection and the opposing surface of the stopper is less than the distance d_c. As a result, the electric double layers are formed in these areas. In the n-th projection, the area where the electric double layer is formed is a circle with the radius r_n give by the next equation:

$$r_n = \sqrt{2R(d_c - d_n) - (d_c - d_n)^2} \quad . \tag{20}$$

As the first approximation, we calculate the electrostatic force F_n working in the electric double layer formed by the n-th projection and the stopper by eq.(21), i.e. we replace the part of the spherical surface where the double layer is formed with a plane opposing to the stopper with a distance $(d_n+d_c)/2$ from it.

$$F_n \cong \frac{\varepsilon_0 \pi r_n^2 V_c^2}{2\{(d_n+d_c)/2\}^2} \tag{21}$$

The total electrostatic force is calculated by adding F_n over all projections where the formation of the electric double layer is possible. When the height h of the projections is 15nm, the period λ of the projection array is 150nm and the contact potential difference V_c is 1V, the surface force was estimated to be from 10^{-7}N to 10^{-6}N. Since this calculated value is enough small compared with the observed surface force (>1.6×10^{-5}N) when the movable plate adhered to the fixed electrode in the fabricated microstructure, the contribution of the electrostatic force due to the contact electrification of the stopper and the fixed electrode to the total surface force is negligible compared with that of the van der Waals force, the capillary force and the hydrogen bonding force.

4. Discussions

From the above study, we found that the van der Waals force, the capillary force and the hydrogen bonding force can generate the surface forces whose magnitudes are included in the surface force range observed in the fabricated microstructure or near to it.

On the other hand, in our previous experiments, by the treatments to reduce physisorbed water molecules on the device surface such as a heating of the device (180℃) and a chemical surface modification to achieve hydrophobic surfaces (HMDS treatment), the surface force could be reduced in major samples and the number of samples in which the movable plate adheded to the fixed electrode was decreased[5].

According to the above study on the van der Waals force, it is expected that this force increases with decreasing the thickness of the water film formed in the gap between the insulator and the metal, since the water has a shield effect for the van der Waals interaction in this system. Taking these results into consideration, it is thought that the capillary force due to the capillary condensation of the water or the hydrogen bonding force between the adsorbed water molecules are dominant in air and the van der Waals force is the major surface force when the physisorbed water molecules on the surface are sufficiently removed. While the relative humidity in which the major surface force changes from the capillary force to the hydrogen bonding force depends on the strength of the interaction between the water molecules and the solid surface, it is thought to be about 60% from observations in the powder technology. Accordingly, the capillary force is dominant in the humidity higher than about 60% and the hydrogen bonding force is the main force in the lower humidity region. Further, when the physisorbed water molecules are sufficiently removed, the van der Waals force becomes dominant instead of them.

Since natural oxide layers are easily formed in air on Si, silicon nitride (Si_3N_4) and usual metals except novel metals, their surfaces are hydrophilic. Therefore, it is thought that the generation mechanism of the surface force in the microstructures fabricated by using Si, SiO_2, Si_3N_4 and the usual metals are same as those in the device investigated in this study.

5. Conclusions

In the microstructure having the movable plate and the counter fixed electrodes with the small gap between them, the magnitude of the surface force which works between them when they contact each other, were investigated theoretically by modeling their contacting parts. The surface forces based on four types of physical forces, i.e. the van der Waals force, the capillary force due to capillary condensed water, the hydrogen bonding force between the adsorbed water molecules and the electrostatic force due to the contact electrification, were studied.

It was found that the van the der Waals force, the capillary force and the hydrogen bonding force can generate the surface forces whose magnitudes are in the range of previously measured surface force or near to it.

It is thought that the dominant surface force is the capillary force when the device is exposed to the high humidity environment and the hydrogen bonding force in thr low humidity condition. When the physisorbed water molecules on the surface are sufficiently removed, the van der Waals force is thought to be the major surface force instead of them.

The electrostatic force due to the contact electrification was enough small compared with the van der Waals force, the capillary force and the hydrogen bonding force. Therefore, its contribution to the surface force is assumed to be negligible.

References

1) H. Guckel, J.J. Sniegowski, T.R. Christensen, S. Mohney, T.F. Kelly: Fabrication of Micromechanical Devices from Polysilicon Films with Smooth Surfaces, Sensors and Actuators, **20**,117/122 (1989)

2) P. Scheeper, J.A. Voorthuyzen, and P. Bergveld: Surface Forces in Micromachined Structures, Proc. Micromechanics Eourope'90, 47/52 (Berlin, November 1990)
3) Y. Tai and R.S. Muller: Friction Study of IC-processed Micromotors, Sensors and Actuators, **A21**-**A23**, 180/183 (1990)
4) M. Mehregany, S.M. Phillips, E.T. Hsu, and J.H. Lang: Operation of Harmonic Side-Drive Micromotors Studied through Gear Ratio Measurements, Tech. Digest. 6th Int. Conf. Solid-State Sensors and Actuators, 59/62 (San Francisco, CA, June 1991)
5) S. Tsuchitani, S,Suzuki, S. Shimada, M. Miki, M. Matsumoto, and S. Kuragaki, Measurement of the Surface Force in Micro Structures and Its Reduction (In Japanese), Trans. of Society of Instrumentation and Control Engineering (SICE), **30**-2, 136/142 (1994)
6) W.C. Heins, Aerozol Technology, Chapter6, Inoue-shoin (1985)
7) K. Okuyama, H. Masuda, K. Higashitani, M. Chikazawa, and T. Kanazawa, Interaction between Two Particles (In Japanese), J. of the Society of Powder Technology, Japan (SPTJ), **22**-7, 451/475 (1985)
8) F. London: The General Theory of Molecular Forces, Trans. Faraday Soc., **33**, 8/26 (1937)
9) H.C. Hamaker: The London van derWaals Attraction between Spherical Particles, Physica, **4**, 1058/1072 (1937)
10) R.A. Fisher: On the Capillary Forces in an Ideal Soil; Correction of Formulae given by W.B. Haines, J. Agric. Sci., 16, 492/505 (1926)
11) M. Chikazawa, T. Kanazawa and T. Yamaguchi: The Role of Adsorbed Water on Adhesion Force of Powder Particles, KONA, Powder Science and Technology in Japan, **2**, 54/61 (1984)
12) M. Shimbo: Silicon to Silicon Direct Bonding Method (In Japanese), Oyo Buturi, **56**-3, 373/376 (1987)
13) Kobunshigakkai, Handbook of Static Electricity (4th edition), Chapter 1, Chijin-shokan (1971)
14) A. Katsunishi, Present Condition and Future of Basic Theory of Electrification (In Japanese), Proc. of Institute of Electrostatics Japan (IESJ), **1**-1, 46/51 (1977)
15) R.A. Erb: Wettability Metals under Continuous Condensing Conditions, J. Phys. Chem., **69**-4, 1306/1309 (1965)
16) W.R. Harper: The Volta Effect as a Cause of Static Electrification, Proc. Roy. Soc., **A205**, 83/103 (1951)

Shigeki TSUCHITANI (Member)

Shigeki Tsuchitani received B.Eng. and M.Eng. degrees in material physics from Osaka University in 1977 and 1979, respectively and received Dr.Eng. in electronic physics from Tokyo Institute of Technology in 1994. In 1979, he joined Hitachi Research Laboratory, Hitachi Ltd. and he had been engaged in research and development of various sensors. Since1996, he has been with the Department of Optomechatronics in Wakayama University, where he is presently an Associate Professor. His research interest includes micro tribology and high density recording using scanning probe microscopes.

Seiko SUZUKI (Member)

Seiko Suzuki received B.Eng. degree from Kinki University in 1965. In 1965, he joined Hitachi Research Laboratory, Hitachi Ltd. Since then, he has been engaged in research and development of sensors for automobile such as air flow sensor, silicon pressure sensor and silicon accelerometer.

Masahiro MATSUMOTO (Non-member)

Masahiro Matsumoto graduated Ehime prefectural Matsuyama technical high school in 1983. Since 1983, he has been working in Hitachi Research Laboratory, Hitachi Ltd. and engaged in research and development of sensors for automobile such as optical fiber gyroscope, ground velocity sensor and silicon accelerometer.

Masayuki MIKI (Non-member)

Masayuki Miki graduated Ibaraki prefectural Katsuta technical high school in 1971. In 1971, he joined Hitachi Research Laboratory, Hitachi Ltd. and engaged in research and development of sensors for automobile such as air flow sensor, air-fuel ratio sensor and silicon accelerometer. Scince 1996, he has been working in Automotive Product Group, Hitachi Ltd.

Reprinted from Trans. of the SICE, Vol.32, No.5, 637/645 (1996)